This is an extended version of the paper presented in SEE7 conference, peer-reviewed again and approved by the JSEE editorial board.

Relations between Liquefaction Resistance and Shear Wave Velocity as Affected by Aging of Sand Deposits

Roozbeh Safaeian Amoly[1*], Kenji Ishihara[2], and Huriye Bilsel[3]

1. Ph.D. Candidate, Civil Engineering Department of Eastern Mediterranean University, North Cyprus, Mersin 10, Turkey, * Corresponding Author; email: rsamoly@gmail.com
2. Professor, Research and Development Initiative of Chou University, Tokyo, Japan
3. Associate Professor, Civil Engineering Department of Eastern Mediterranean University, North Cyprus, Mersin 10, Turkey

Received: 19/08/2015
Accepted: 16/12/2015

ABSTRACT

Since shear wave velocity is determined by non-destructive experiments in the narrow range of small strain, some researchers have reservations about employing it in the assessment of medium-to-large phenomenon, i.e. liquefaction. However, some others confirm that the shear wave velocity is more likely to suit for distinguishing the liquefaction and non-liquefaction susceptibility of sand deposits by means of the chart correlating liquefaction resistance to shear wave velocity, similar to the other types of indices, i.e. SPT and CPT, despite of its few limitations. Such liquefaction charts have commonly been proposed based on the liquefaction resistance of young Holocene deposits, without taking "age" into account. In an attempt to bridge the gap between those ideas, relations between liquefaction resistance and shear wave velocity of sand deposits are proposed under aging effect using a newly introduced index property, i.e. "cyclic reference strain" or "cyclic yield strain", to differentiate between new and old sand deposits. The smaller the cyclic yield strain, the less ductile response of soil and vice versa. It may be concluded, therefore, that this parameter can be employed as a criterion for taking into account the cementation or the effect of age in sandy soils.

Keywords:
Aging effect; Liquefaction resistance; Shear wave velocity; Cyclic yield strain

1. Introduction

Youd and Hoose [1] and Youd and Perkins [2], the first pioneers recognized that the liquefaction resistance of sandy deposits increases noticeably with geological age, indicated that the older sediments of Pre-Pleistocene and Pleistocene epoch are essentially more resistant to liquefaction than the younger sediments belonged to Holocene epoch. Seed [3] pointed out that the liquefaction resistance of undisturbed specimens extracted from a fill deposited during 1000 years over that of freshly deposited specimens of the same sand increases approximately 50-100%. Kokusho et al. [4] observed that the cyclic strength resistance of undisturbed Narita sand relative to the cyclic resistance of freshly reconstituted laboratory samples reaches up to 80%. Troncoso et al. [5] reported on the order of 200-350% gain in cyclic resistance of undisturbed sandy specimens, obtained from two tailings dam locations at El Cobre in Chile with various ages of 1, 5, 30 years, relative to freshly deposited specimen in laboratory. It should be noted that the preceding studies had not directly considered the aging effect

along with any soil indices such as shear wave velocity, CPT and SPT.

On the other hand, the empirical correlation between the liquefaction resistance and shear wave velocity as in-situ index, which is presented by Andrus and Stokoe [6], is based on the liquefaction of sandy deposits dating back to young Holocene epoch. The empirical correlation has been developed by many researchers such as Kayen et al. [7], Zhou and Chen [8], Baxter et al. [9] and Kayen et al. [10], without any particular consideration of the age of deposits in which experiments were carried out.

In an attempt to fill the gap in understanding the relationship between the shear wave velocity involving small strain and the cyclic resistance of sandy soils inducing medium to large shear strain, what might be termed "cyclic yield strain", or "cyclic reference strain" is introduced as a factor that may reflect the effect of aging on sandy deposits in order to identify new or liquefied deposits as well as un-liquefied old deposits in the same chart.

Several factors may be envisaged to exert influence on the ductility or brittleness of soils. One of the factors, likely to be associated, would be the aging of soil deposits. It is with good reasons to infer that in-situ soils having a long history of deposition may show "brittle" behaviour, in contrast to the "ductile" response of soils with a short history of deposition. Thus, the effect of aging of soil deposits may be reflected somewhat upon the cyclic yield strain. In view of the fact that the larger the cyclic yield strain, the more ductile the response of soils would be and vice versa, it may be concluded that the cyclic yield strain can be utilized as a yardstick parameter for taking into account the aging effect of sandy soils. It is reasonably conceived that the cyclic yield strain will take larger values for ductile fresh deposit and smaller values for brittle old aged deposits of sands.

The principal aim of this paper is to propose a new procedure that takes into account the relation between liquefaction resistance and shear wave velocity in terms of aging effect by means of the cyclic yield strain or the cyclic reference strain.

2. The Concept of "Cyclic Yield Strain" or "Cyclic Reference Strain"

To measure the liquefaction resistance of sandy soil, the cyclic triaxial experiments are conducted 2-4 times by various cyclic stress ratio, $R_L = \sigma_d / (2\sigma'_0)$, where σ_d and σ'_0 denote a single amplitude of axial stress and initial confining stress, respectively. For instance, a particular cyclic stress ratios, e.g. $R_L = 0.20$, applied to the sample, as shown in Figure (1a), in order to produce different values of single amplitude of axial strain, ε_a, i.e. 0.75%(a'), 1.25%(b'), 2.5%(c'), 5%(d'). After similar experiments are repeated with several cyclic stress ratios, a set of curved lines is obtained by connecting the points of the same axial strain amplitude as shown in Figure (1a).

It should be noted that 100% pore pressure build-up occurs almost concurrently with 2.5% single amplitude of axial strain, and 10 or 20 cycles of uniform loading can be representative of the strong earthquake with a magnitude of 7½. Thus, it has been customary to perceive the cyclic stress ratio, which is intersection of 2.5% curved line at 20th cycle, assuming as liquefaction triggering. To intersect a line perpendicular to number-of-cycle axis at twentieth cycle, and four curved lines, passing through points, i.e. a, b, c and d, are made as a function of the particular cyclic stress ratio, $R_L = 0.15$, as shown in Figure (1a). Then, it is feasible to set up by connecting those points in the plot of cyclic stress ratio versus axial strain, as shown in Figure (1b), which can generally be considered as a kind of non-linear stress-strain model.

Based on the elasto-plastic theory, bi-linear lines can approximately be a representative of the non-linear stress-strain relation. As shown in Figure (1b), elastic behavior is related to the line which passes through zero point with slop, G_0, and plastic behavior is associated with the line which is the level of particular cyclic stress ratio, $R_L = 0.15$. The corresponding axial strain of point *B*, which results from intersection of tangent and asymptotic lines, may be considered as a kind of "reference strain" or "yield strain" in cyclic loading. Based on Figure (1b), cyclic yield strain, ε_{ay}, can be defined by Eq. (1) in order to make this strain non-dimensional format, atmospheric pressure, $P_a = 98$ kN/m^2, multiplied by the cyclic stress ratio.

$$\varepsilon_{ay} = \frac{R_L \cdot p_a}{G_{01}} \tag{1}$$

where, G_{01} denotes the value of G_0 at the

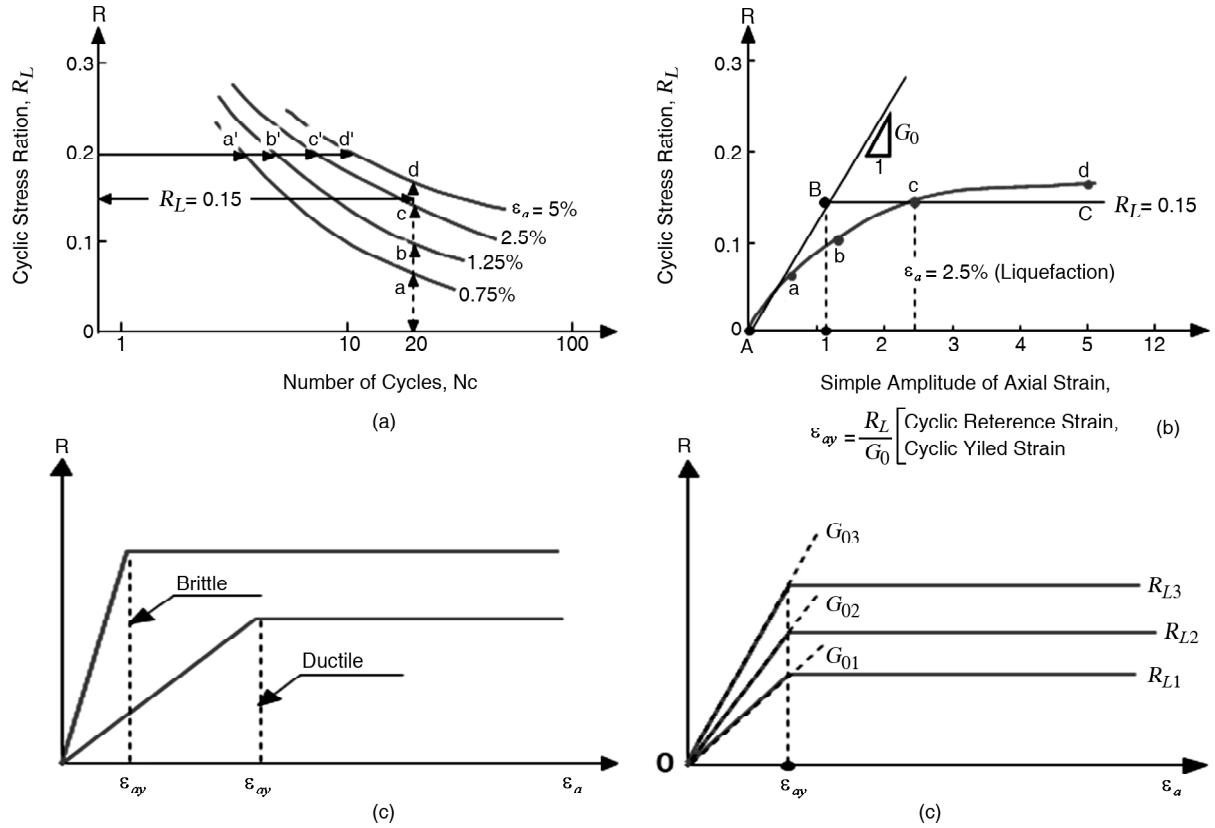

Figure 1. Schematic diagrams of the yield strain in cyclic loading.

atmospheric pressure. The physical interpretation of cyclic yield strain is shown in Figure (1c). That is, if the value of ε_{ay} is small, the soil is considered as a material with "brittle" behavior, which may be indicative of old age deposits. The soil is deemed as "ductile" behavior if the value of ε_{ay} is large, which can be representative of the new age deposits. The level of ductility or brittleness for a particular soil could be the same if the value of ε_{ay} remains constant as shown in Figure (1d).

3. The Correlation of Cyclic Yield Strain and Shrear Wave Velocity

Based on the dynamic property of soil, the initial shear modulus, G_0, can be derived from shear wave velocity, V_S, by Eq. (2). Since shear modulus at atmospheric pressure, G_{01}, is utilized in Eq. (1), shear wave velocity should be normalized to V_{S1} by being multiplied by $(P_a/\sigma'_v)^{0.25}$, where σ'_v = effective overburden pressure at a particular depth, g = 9.8 m/sec^2 and ρ = bulk unit weight.

$$G_{01} = \frac{\rho}{g} V_{s1}^{\ 2} \tag{2}$$

Substituting Eq. (2) into Eq. (1) yields Eq. (3), which can practically be utilized in the evaluation of cyclic yield strain.

$$\varepsilon_{ay} = \frac{R_L \cdot p_a}{G_{01}} = \frac{R_L \cdot p_a}{\rho/g \cdot V_{s1}^{\ 2}} \tag{3}$$

4. Undisturbed Specimens for Measuring Cyclic Yield Strain

To determine the value of cyclic yield strain, ε_{ay} a large number of tests were carried out in the field as well as in the laboratory on undisturbed and disturbed specimens. For this aim, the area of Asahi city in Chiba, which is along the costal line of Pacific Ocean, is shown in Figures (2) and (3). Moreover, Ohya tailings dam site located in northeast of Japan is shown in Figures (2), (5) and (6). Detailed account of soil conditions and features of failure in tailings dams are described in a paper by Ishihara et al. [11]. Both of them, affected by the 2011 East Japan earthquake, have been considered as earthquake-induced liquefaction zones in this study.

Soil borings were carried out at six selected locations of Asahi city as shown in Figure (3). Thus,

six detailed soil profiles were obtained on the basis of geotechnical investigation, three of which are shown in Figures (4a), (4b) and (4c). In order to extract undisturbed specimens, three different samplers, the thin-wall tube sampler, the triple tube sampler and the Denison sampler, are utilized based on the depth and the type of soil.

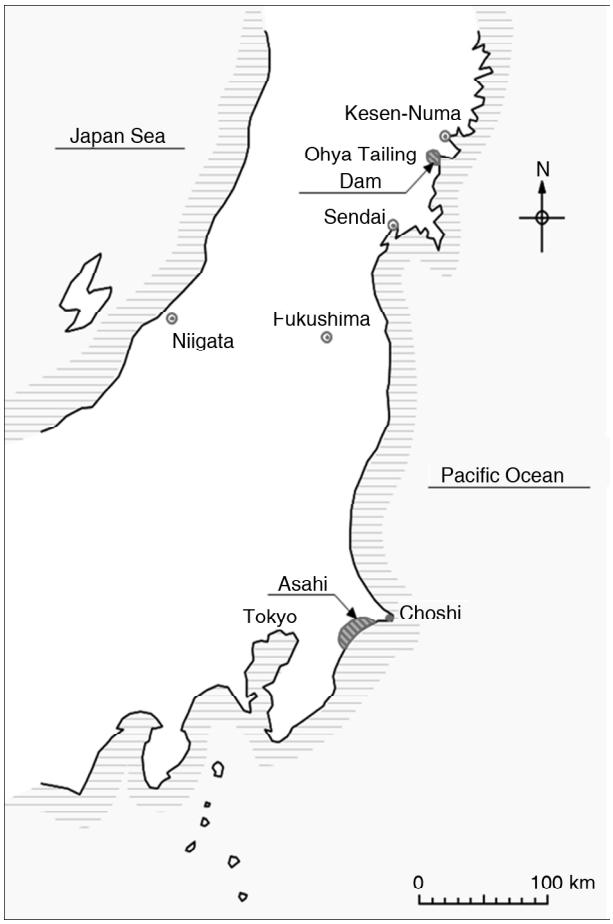

Figure 2. Asahi site for sampling location.

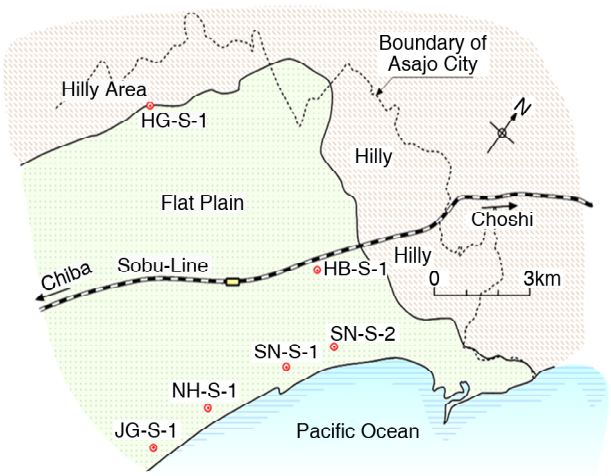

Figure 3. Locations of bore holes in Asahi site.

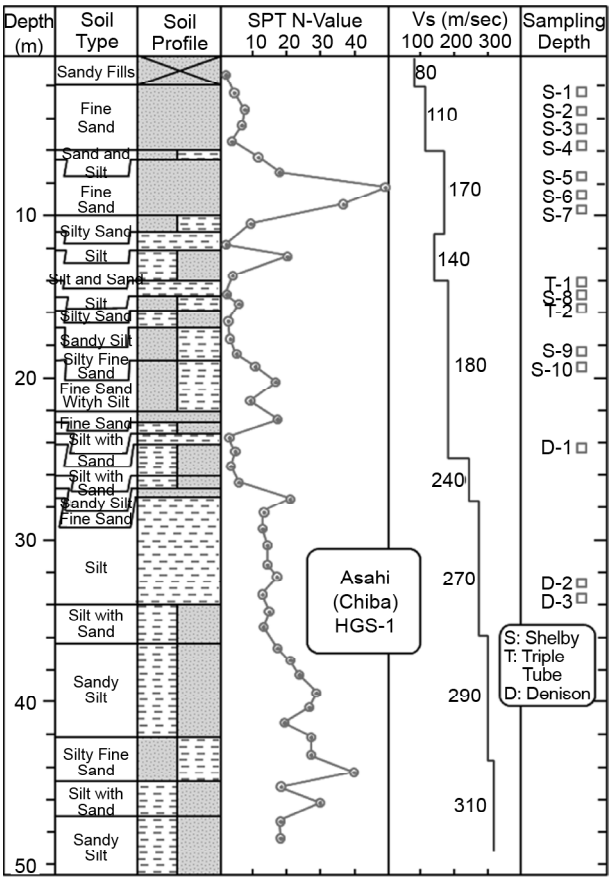

Figure 4a. Soil profile at the site of sampling in Asahi (HG-S-1).

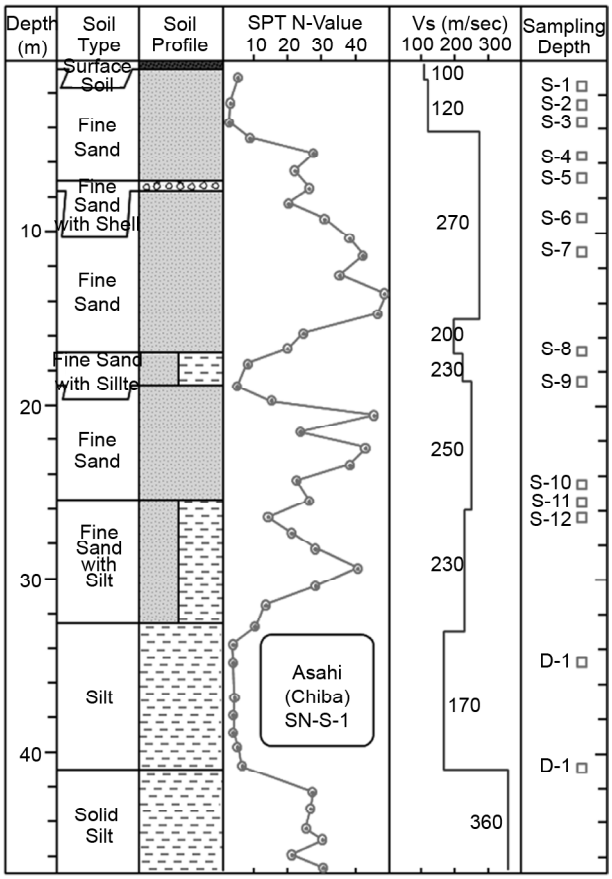

Figure 4b. Soil profile at the site of sampling in Asahi (SN-S-1).

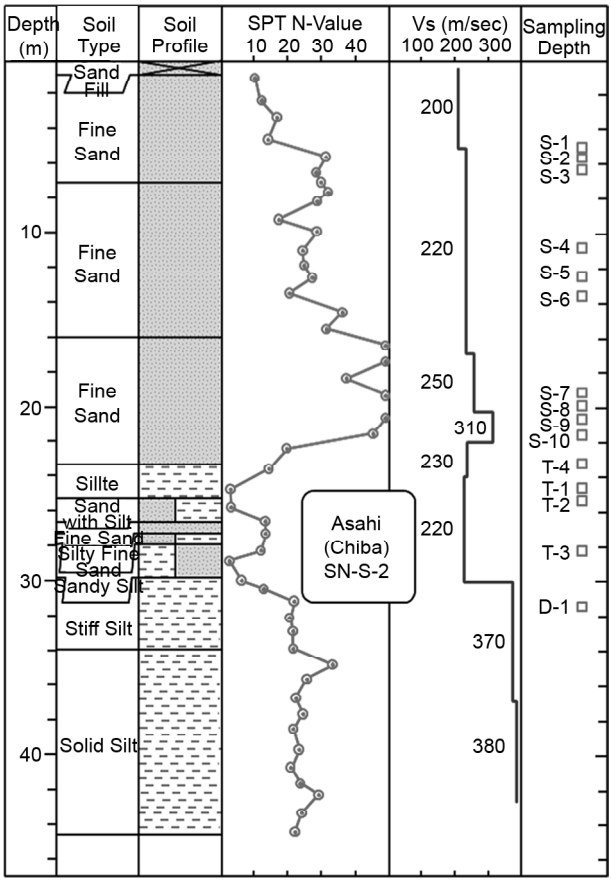

Figure 4c. Soil profile at the site of sampling in Asahi (SN-S-2).

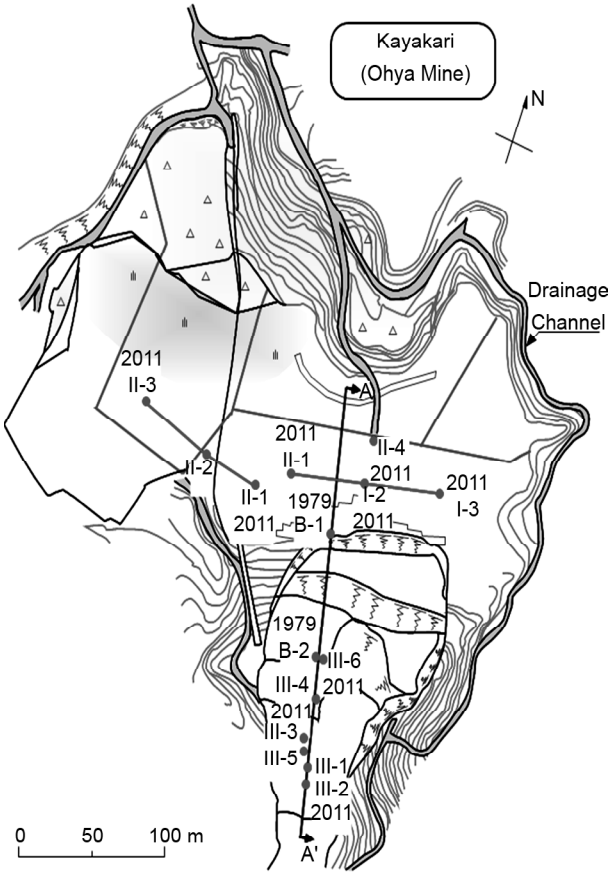

Figure 5. Plan view of the failed tailings dam at Ohya mine.

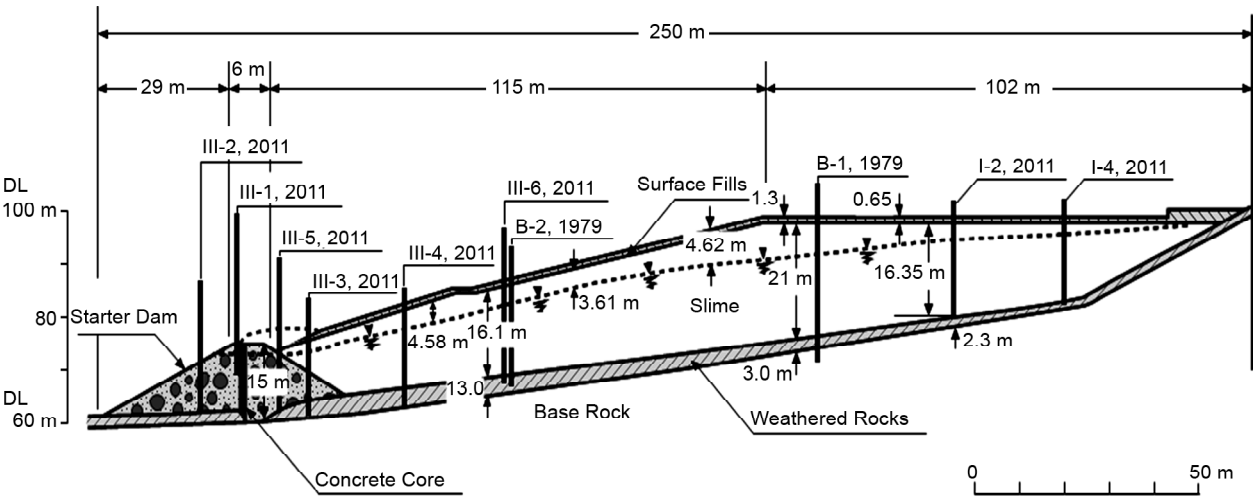

Figure 6. Cross section of the failed tailings dam at Ohya mine showing the locations of boring logs in 1979 and 2011.

5. The Procedure of Cyclic Triaxial Test and Vs Measurement in Laboratory

Tube samples from Asahi site contained about 30% fines and thus were hung vertically overnight at the site to drain excess water. The partially saturated sands in the tubes were frozen in the field.

For setting up the sample, the frozen sample enclosed in a rub membrane, 100 mm long and 50 mm in diameter, was placed to the chamber of cyclic triaxial apparatus between the pedestal and the top cap after measuring the weight, the length (twice), and the diameter (six times), i.e. twice on the bottom, the middle and the top of the sample.

For thawing, the sample was permitted to thaw for approximately 1-2 hours while a slight 20 kN/m^2 vacuum was previously employed to keep the

general sample shape constant. After having completely thawed, the diameter of the sample was measured for six times with Vernier Caliper. Next, the triaxial cell was set up around the sample and the water was then permitted to enter the triaxial chamber. In this step, the vacuum was slowly decreased to zero while the cell pressure was simultaneously decreased to the value of 20 kN/m^2.

For carbon dioxide percolation, it was permitted to percolate gradually into the sample for 30-60 minutes, depending on the amount of fine content, by opening the drainage valves of the pedestal platen and the top cap, in order to be replaced with the air and water in the sample.

For saturation and checking B-value, let the de-aired water in the sample for approximately 30-60 minutes, or the 300 ml of that were run through it, in order to fill up all voids so that the sample becomes well-saturated. Next, a 200 kN/m^2 back pressure was gradually employed while the cell pressure was automatically increased with 20 kN/m^2 difference. Applying the back pressure lasted approximately 10 minutes at constant differential head because of better saturation. Then, the B-value of the sample, the ratio of the pore water pressure to cell pressure, quantified by 50 kN/m^2 increase in cell pressure and measuring the change of the pore water pressure from the bottom of the sample by means of the transducer of water pressure. Based on JGS, the saturation of the sample is satisfactory, provided that the B-value becomes more than 0.96.

For consolidation and cyclic triaxial test, it was permitted to isotropically be consolidated to a specified effective confining pressure resulting from the difference between the cell pressure and back pressure, which is dependent on the depth of undisturbed sample in soil profile. As soon as the consolidation of the sample was fully accomplished in a drained condition for approximately 30-90 minutes, the sample was subjected to cyclic axial load in the form of 1 Hz sinusoidal wave in un-drained condition until the axial deformation of the sample reached up to 10%. Throughout cyclic loading, the values of the change in pore water pressure, axial deformation and axial load were automatically recorded with constant cell pressure.

For the V_S measurements, the cyclic triaxial was capable of the shear wave velocity measurement by means of a new device by which torsional impulses sent off from the top cap were received in the pedestal platen, thereby monitoring the transmission time thorough the sample height by which the *VS* were calculated. In this experiment, the *VS* was measured twice after these steps, i.e. consolidation, liquefaction in un-drained condition and approximately 30-60 minutes after opening drainage value.

6. Outcomes of Experiments on Undisturbed Specimens

The outcomes of cyclic loading experiment on the undisturbed specimens from Asahi site are shown in Tables (1) and (2), and those from Ohya tailings dam site are depicted in Table (3). Some of experiments were carried out by Chiba Eng. Co. without V_S measurement in the laboratory as shown in Table (1). Consequently, V_S values of in-situ measurement are utilized, whereas the value of V_{S1} related to laboratory measurements was calculated by the value of G_{01} measured by laboratory tests. Moreover, V_S measurements in the field were performed by Kiso-Jiban consultants Co. in Ohya tailings dam site as illustrated in Table (3). However, some other experiments were performed by Kiso-Jiban consultants Co. with V_S measurements in laboratory as illustrated in Table (2), and the values of V_{S1} related to laboratory and field measurements was calculated by the values of V_S measured by Laboratory and field tests. In Ohya dam site, in-situ V_S measurements were also carried out by Kiso-Jiban consultants Co.

In Tables (1) to (3), specimens related to fills or once-liquefied alluviums are separated from those associated with non-liquefied alluvial and diluvial or old deposits. Moreover, in the columns of V_S and V_{S1} , laboratory measurements of V_S are distinguished from field measurements by denoting "*L*" and "*F*" as laboratory and field, respectively. In Tables (1) to (3), the once-liquefied deposits or fills are denoted by "ℓ" and non-liquefied old deposits are denoted by "*n*".

7. Cyclic Strength Versus Shear Wave Velocity for Reconstituted Samples

7.1. Cyclic Strength Versus V_{S1} for Reconstituted Samples from Asahi Sand

After the series of tests were finished for the

Table 1. Undisturbed specimens from Asahi with Vs measurement in the field.

Site	Sample Number	Age	Depth (m)	σ'_v (kpa)	*N*-value	*N*1-value	*FC* (%)	*Vs* (m/sec)	Vs_1 (m/sec)	G_{01} (Mpa)	R_L	$\varepsilon_{ay} = \frac{R_L \cdot p_s}{G_{01}}$
HB-S-1	HB-S-1 (S-1)	$Fill^{\ell}$	1.0-3.8	30	7	9	0.9	F160	L168 F216	L52.2 F86.3	0.304	L** 5.82×10^{-4} F* 4.48×10^{-4}
	HB-S-1 (S-4)	As^{n}	7.0-10.9	87	25	27	1	F240	L189 F248	L65.7 F116.0	0.282	L 4.29×10^{-4} F 2.43×10^{-4}
	HB-S-1 (S-7)	As^{n}	15.0-16.9	150	21	26	10.7	F190	L201 F172	L76.4 F55.8	0.276	L 3.61×10^{-4} F 4.95×10^{-4}
	HB-S-1 (S-9)	As^{n}	22.0-23.7	215	12	8	9.6	F190	L208 F157	L81.8 F46.5	0.276	L 3.37×10^{-4} F 5.94×10^{-4}
JG-S-1	JG-S-1 (S-1)	As^{n}	5.0-8.0	74	25	29	2.2	F180	L150 F194	L42.9 F71.1	0.176	L 4.10×10^{-4} F 2.48×10^{-4}
	JG-S-1 (S-4)	As^{n}	8.0-9.9	91	22	23	6.6	F150	L168 F154	L53.1 F44.5	0.268	L 5.05×10^{-4} F 6.02×10^{-4}
	JG-S-1 (S-6)	As^{n}	16.0-17.8	163	45	35	5.7	F270	L192 F239	L69.6 F108.0	0.28	L 4.02×10^{-4} F 2.59×10^{-4}
	JG-S-1 (S-8)	Ds^{n}	26.0-27.8	248	11	7	28.7	F250	L179 F199	L73.4 F74.8	0.229	L 3.12×10^{-4} F 3.06×10^{-4}
NH-S-1	NH-S-1 (S-1)	$Fill^{\ell}$	2.0-5.8	53	4	6	20.5	F140	L121 F164	L27.3 F50.1	0.295	L 10.8×10^{-4} F 5.89×10^{-4}
	NH-S-1 (S-4)	As^{n}	10.0-11.9	112	31	30	9.6	F260	L199 F253	L75.3 F122.0	0.206	L 2.73×10^{-4} F 1.69×10^{-4}
	NH-S-1 (S-6)	Ds^{n}	26.0-27.0	244	4	3	84	F150	L165 F120	L51.4 F27.2	0.246	L 4.78×10^{-4} F 9.04×10^{-4}

L: Laboratory, *F*: Field, ℓ : Liquefied Alluviums or Fills, *n*: Non Liquefied, *As*: Alluvial Sand, *Ds*: Diluvial Sand

Table 2. Undisturbed specimens from Asahi with Vs measurement in the laboratory.

Site	Sample Number	Age	Depth (m)	σ'_v (kpa)	*N*-value	N_1-value	*FC* (%)	Vs_1 (m/sec)	Vs_1 (m/sec)	G_{01} (Mpa)	R_L	$\varepsilon_{ay} = \frac{R_L \cdot p_s}{G_{01}}$
HB-S-1	HG-S-1 (S-1)	As^{ℓ}	2.0-3.0	25	4	6	11.8	L127 F110	L 180 F 156	L 59.5 F 47.6	0.23	L** 3.86×10^{-4} F* 4.83×10^{-4}
	HG-S-1 (S-4)	As^{ℓ}	4.0-5.0	60	6	8	12.1	L115 F115	L 131 F 131	L 31.5 F 31.5	0.3	L 9.52×10^{-4} F 9.52×10^{-4}
	HG-S-1 (S-1)	As^{n}	4.0-6.0	60	6	8	25.4	F110	F 125	F 28.7	0.299	F 10.4×10^{-4}
	HG-S-1 (S-5)	As^{n}	7.0-10.0	87	18	19	26.2	F170	F 176	F 45.4	0.281	F 4.80×10^{-4}
	HG-S-1 (S-11)	Ds^{n}	18.0-20.0	180	10	7	52.4	F180	F 155	F 26.7 F 45.4	0.284	F 6.25×10^{-4}
	HG-S-1 (S-11)	Ds^{n}	18.0-20.0	180	10	7	42.3	L138 F180	L 119 F 155	L 61.9 F 45.4	0.28	L 10.5×10^{-4} F 6.17×10^{-4}
JG-S-1	SN-S-1 (S-6)	$Fill^{\ell}$	1.0-2.0	20	5	11	1.9	L121 F100	L 181 F 149	L 61.9 F 41.7	0.35	L 5.65×10^{-4} F 8.39×10^{-4}
	SN-S-1 (S-10)	Ds^{n}	24.0-26.1	215	23	16	9	L211 F220	L 174 F 182	L 57.8 F 66.3	0.24	L 4.15×10^{-4} F 3.62×10^{-4}
NH-S-1	SN-S-2 (S-6)	As^{n}	13.0-14.0	115	26	24	5	L209 F220	L 202 F 182	L 76.3 F 84.8	0.23	L 3.01×10^{-4} F 2.71×10^{-4}
	SN-S-2 (S-7)	As^{n}	20.1-20.8	190	79	57	1.3	L218 F250	L 186 F 213	L 65.3 F 86.4	0.22	L 3.37×10^{-4} F 2.55×10^{-4}
	SN-S-2 (S-9)	As^{n}	20.8-21.8	198	79	57	5	L134 F250	L 113 F 211	L 24.1 F 84.0	0.2	L 8.30×10^{-4} F 2.38×10^{-4}

ℓ : Liquefied Alluviums or Fills, *n*: Non Liquefied, *L*: Laboratory, *F*: Field, *As*: Alluvial Sand, *Ds*: Diluvial Sand

Table 3. Tailings dam at Ohya mine (Miyagi prefecture).

Sampling Time	Age	Depth (m)	σ'_v (kpa)	*N*-Value	N_1-value	*FC* (%)	*Vs* (m/sec)	Vs_1 (m/sec)	G_{01} (Mpa)	R_L	$\varepsilon_{ay} = \frac{R_L \cdot p_s}{G_{01}}$
After the 2011 Quake	New^{ℓ}	5.0-5.8	85	3	3.3	66	F140	F146	F40.2	0.18	F4.48×10^{-4}
	New^{ℓ}	12.0-12.8	138	1	0.8	96	F170	F157	F46.5	0.173	F3.72×10^{-4}
	New^{ℓ}	5.0-5.9	88	2	2.1	33	F140	F144	F39.1	0.197	F5.04×10^{-4}
	New^{ℓ}	8.7-9.5	120	1	0.9	96	F150	F143	F38.6	0.179	F4.64×10^{-4}
	New^{ℓ}	12.0-12.8	142	2	1.6	97	F170	F156	F45.9	0.208	F4.53×10^{-4}
	New^{ℓ}	13.1-14.0	160	5	3.6	94	F200	F178	F61.4	0.307	F5.00×10^{-4}
Before the 1977 Quake	Old^{n}	5.80-6.55	106	11	10.5	75	F120	F118	F27.0	0.207	F7.67×10^{-4}
	Old^{n}	18.0-18.8	226	0	0	89	F190	F155	F46.5	0.238	F5.12×10^{-4}
	Old^{n}	5.0-5.8	91	4	4.2	87	F120	F123	F29.3	0.268	F9.15×10^{-4}
	Old^{n}	10.0-10.8	128	3	2.5	92	F240	F226	F98.9	0.231	F2.34×10^{-4}

undisturbed samples from Asahi, the same samples were once mixed, air-dried and reconstituted to test specimens having approximately the same density. The *Vs*-measurements and cyclic loading tests were performed similarly on these reconstituted samples. The results of the tests are illustrated in Table (4).

7.2. Cyclic Strength Versus V_{S1} for Reconstituted Samples from Nagoya Sand

With an aim of examining effects of fines content, a sandy soil from a site in Nagoya was sorted out using the 74μ sieve to separate fines fraction from the silty sand. Then, the fines were mixed with sand fraction to produce silty sands having fines proportions of 10% and 30%. The artificial materials thus produced were used to prepare specimens with a relative density of 50% and 70% and tested in the same fashion using the same apparatus. The results of the tests are listed in Table (5).

8. The Correlation Between the Cyclic Strength and Shear Wave Velocity

Since new fills or liquefied sands are totally different from old age sands in terms of cementation, stiffness and strength, their correlations of cyclic strength and V_{S1} may be separated into two groups. Therefore, the values of V_{S1} , measured in field and laboratory, versus liquefaction resistance were plotted in Figures (7) and (8) in terms of the old

Table 4. Reconstituted specimens from Asahi site.

Specimens	*FC* (%)	*e*	$\frac{e_{max}}{e_{min}}$	*Dr* (%)	Vs_1 (m/sec)	G_{01} (Mpa)	R_L	$\varepsilon_{ay} = \frac{R_L \cdot p_s}{G_{01}}$
HG-S-1 (2.0-3.0 m)	11.8	0.967	1.486 0.863	83.3	177	59.1	0.19	3.21×10^{-4}
HG-S-1 (4.0-5.0 m)	12.1	1.02	1.572 0.929	85.8	135	34.4	0.21	6.10×10^{-4}
HG-S-1 (18.0-19.0 m)	43.09	1.053	1.803 0.931	86	115	24.9	0.12	4.82×10^{-4}
HG-S-1 (19.0-20.0 m)	40.8	1.047	1.581 0.839	72	125	29.5	0.13	4.41×10^{-4}
SN-S-1 (24.0-24.6 m)	13.6	1.152	1.597 0.939	67.6	149	41.9	0.12	2.86×10^{-4}
SN-S-1 (25.3-26.1 m)	4.5	0.89	1.232 0.768	73.3	158	47.1	0.175	3.71×10^{-4}
SN-S-2 (13.0-14.0 m)	5.3	0.837	1.298 0.764	86.3	168	53.2	0.18	3.38×10^{-4}
SN-S-2 (20.1-20.8 m)	0.95	0.695	0.967 0.579	70.1	173	56.4	0.185	3.28×10^{-4}
SN-S-2 (20.8-21.8 m)	5	1.073	1.46 0.829	61.3	105	20.8	0.12	5.77×10^{-4}

Table 5. Reconstituted specimens of Nagoya sand.

Specimens	e	$\frac{e_{max}}{e_{min}}$	Dr (%)	Vs_1 (m/sec)	G_{01} (Mpa)	R_L	$\varepsilon_{ay} = \frac{R_L \cdot p_s}{G_{01}}$
Fine Content 0 %	0.850	1.077 0.623	50	149	41.9	0.22	5.25×10^{-4}
	0.769	1.077 0.623	70	159	47.7	0.28	5.87×10^{-4}
Fine Content 10 %	0.867	1.118 0.616	50	123	28.5	0.14	4.91×10^{-4}
	0.767	1.118 0.616	70	129	31.4	0.27	8.60×10^{-4}
Fine Content 30 %	0.979	1.288 0.671	50	110	22.8	0.10	4.38×10^{-4}
	0.865	1.288 0.671	70	115	24.9	0.15	6.01×10^{-4}

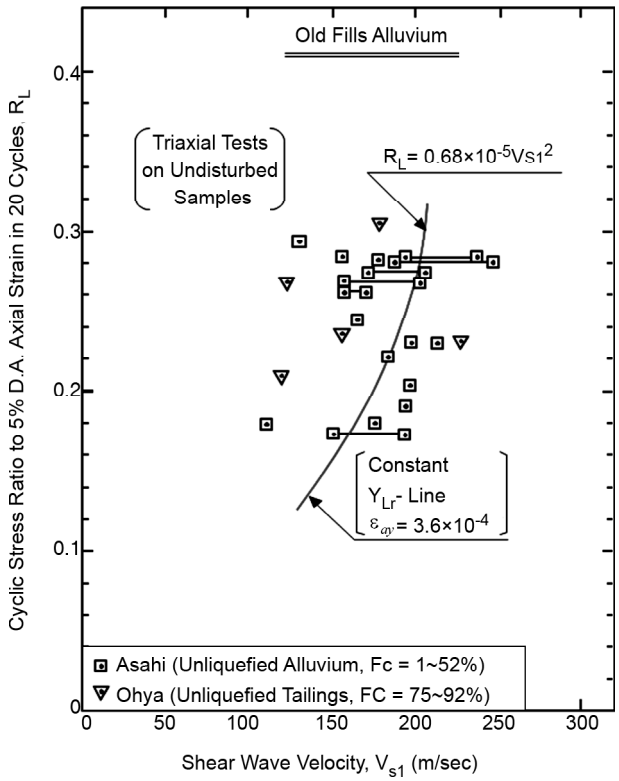

Figure 7. Relation between the cyclic resistance and shear wave velocity for old unliquefied deposits.

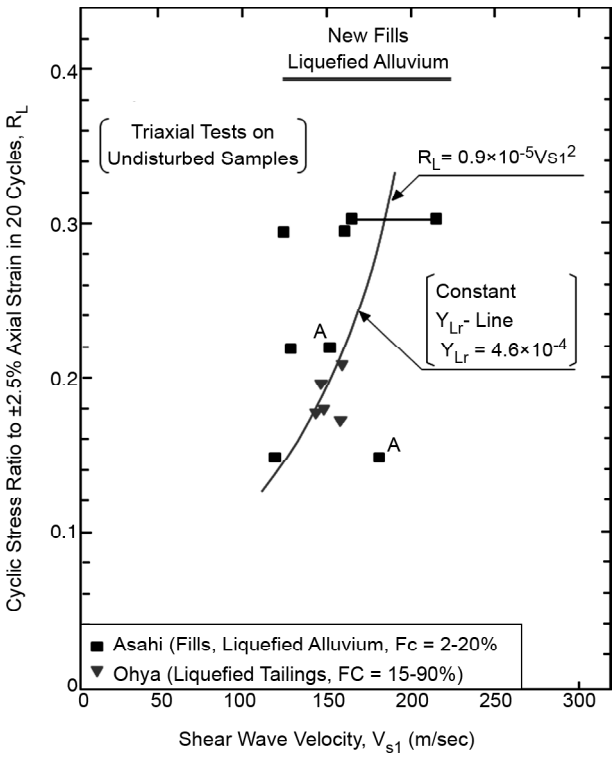

Figure 8. Relation between the cyclic resistance and shear wave velocity for intact samples from new fills and liquefied alluvium.

and new age deposits based on Tables (1) to (3). Regarding the values of V_{S1}, there appears no clearly discernible tendency of differentiating between the data from the field and those from the laboratory tests. Thus, the data from these two sources are joined by a horizontal line connecting the two points in the diagram.

Two distinctive curves may be proposed on the basis of their age by means of the experimental data of Ohya dam site identified by the solid and open reverse triangle symbols, and of Asahi city site identified by the solid and open rectangle symbols in Figures (7) and (8), respectively. The characteristics of these curves are explained below:

1) The chart of cyclic strength versus V_{S1} for old age deposits is presented in Figure (7). The curved line passing through average points of data is represented by $R_L = 0.68\times10^{-5}\ V_{S1}$, and the corresponding cyclic yield strain is (3.6×10^{-4}). With regard to this point, the values of V_{S1} measured in field

and laboratory were given equal weighting. Thus, the proposed line is passed through the average points of in situ and laboratory V_{S1}.

2) The chart of cyclic strength versus V_{S1} for new age deposits based on the undisturbed specimens from the new fills or liquefied sands is presented in Figure (8). The curved line drawn through the average points is represented by $R_L = 0.9\times10^{-5}\ V_{S1}$ and the corresponding cyclic yield strain is 4.6×10^{-6}. Since there were relatively few data to indicate the regression line reliably as shown in Figure (8), a series of experiments was conducted on the reconstituted specimens from undisturbed specimens tested previously in this project, which is identified by the open rectangle symbol "△", and Nagoya sand with various fines contents, i.e. 0%, 10% and 30%, which is identified by the solid reverse rectangle symbol "▼" in terms of RL versus V_{S1}. The results of those specimens as shown in Figure (9) are accurately consistent with the proposed line.

9. The Correlation Between Liquefaction Resistance and Shear Wave Velocity for New and Old Aged Deposits

The curve in Figure (7) can be representative of old age deposits as shown in Figure (10) along with the curve related to new age deposit in Figure (8). It may be concluded that the corresponding value of new deposits, $\varepsilon_{ay} = 4.6\times10^{-4}$, is greater than the value of $\varepsilon_{ay} = 3.6\times10^{-4}$ for old deposit. This inferred, as shown Figure (1c), the newly artificial deposits are associated with more of ductile feature in comparison to brittle behavior of old age deposits.

There are several deterministic charts proposed for the relationship between the cyclic strength and shear wave velocity V_{S1}. These are summarized by Andrus and Stokoe [6] as reproduced in one diagram. The two lines proposed in the present study are superimposed in Figure (10). It appears that the majority of the data sets complied hitherto are those from field observations and measurements. The proposed curve pertaining to old deposits with $\varepsilon_{ay} = 3.6\times10^{-4}$ seems to show a reasonable level of coincidence particularly with the relations proposed by Tokimatsu and Uchida [13] and Robertson et al. [12] in Figure (10).

Moreover, there are several probabilistic charts suggested for the correlation between the cyclic resistance and shear wave velocity V_{S1}, among

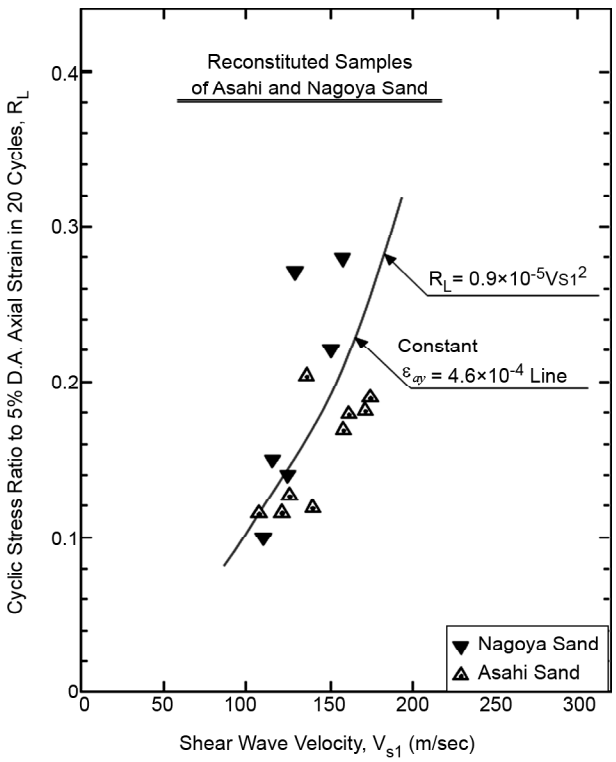

Figure 9. Relation between the cyclic resistance and shear wave velocity for disturbed or reconstituted samples.

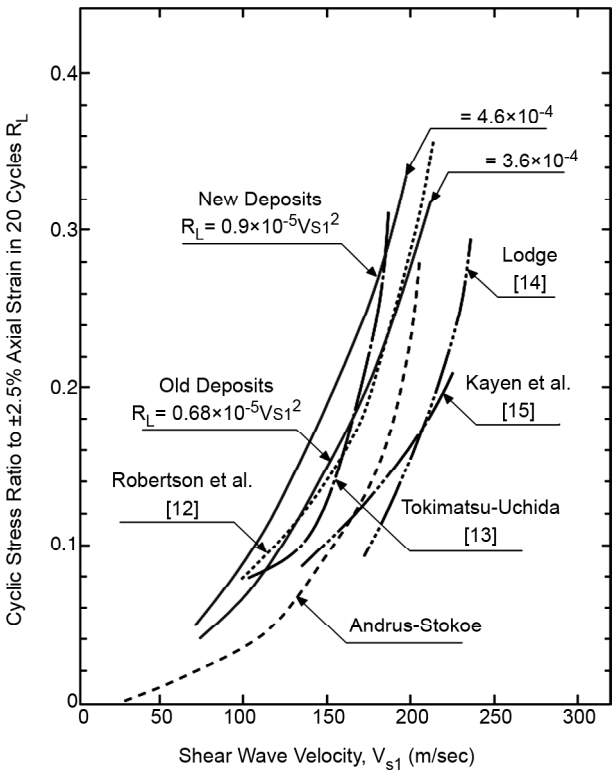

Figure 10. Summary curves of the liquefaction resistance versus shear wave velocity for newly deposited and old deposits of sandy soils (Reproduced from the figure by Andrus and Stokoe [6]).

which Kayen et al. [7] is highly consistent with the outcomes of this study. For instance, Kayen et al. [7] proposed the probabilistic chart based on gathering together a global *Vs* database based on in-situ measurement of *Vs* from all over the world, Figure (11). By superimposing the two curved lines of this study on this chart, the curved line related to new deposits falls between two levels of liquefaction potential, P_L = 50% and 80%, while the curved line for old deposits is between P_L = 20% and 50%. Therefore, the liquefaction susceptibility of new deposits is higher than 50%, whereas that of old deposits is lower than 50%. In the present study, two methods of liquefaction assessment, one based on deterministic evaluation and the other based on probabilistic evaluation of in-situ measurement, are mutually confirmed.

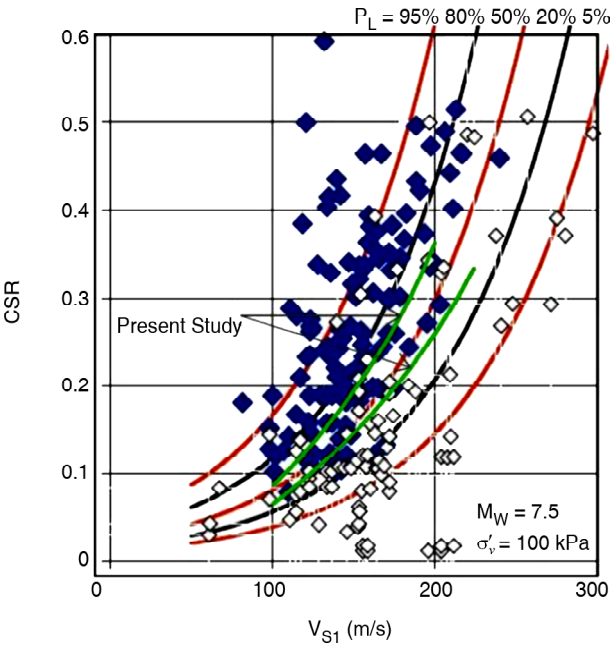

Figure 11. Curved lines of the present study along with preliminary probabilistic liquefaction onset contours determined by processing of 60% of the global Vs1data set to date [7].

10. Conclusions

An attempt was made to examine if it is appropriate or not to make use of a single unique relationship for the cyclic strength of sandy soils as correlated with the shear wave velocity. As one of the factors, effects of aging were investigated in this paper by using the cyclic triaxial test apparatus. The tests were performed on undisturbed samples recovered from in-situ deposits of known liquefaction and also on samples from deposits of known non-liquefaction at the time of the 2011 East Japan Earthquake. In parallel to this, similar series of tests were carried out on reconstituted samples of several sandy soils. The tests consisted of non-destructive type measurements of shear wave velocity first, followed by the cyclic loading to cause liquefaction. By taking the ratio between the cyclic resistance to cause liquefaction in 20 cycles and the square of the shear wave velocity, what might be called "cyclic yield strain" or "cyclic reference strain" was defined.

It was indicated that the value of cyclic yield strain is directly proportional to ductile behavior of soil. That is, the higher the cyclic yield strain, the higher the ductile nature of the soil can be. It may be concluded, therefore, that the cyclic yield strain may be a relevant parameter to correlate the age of deposits in terms of ductility or brittleness. It may also be noted that along with utilizing common correlation of cyclic strength versus shear wave velocity, the multiple curves are separately established to take into account the age of deposits.

References

1. Youd, T.L. and Hoose, S.N. (1977) Liquefaction susceptibility and geologic setting. *Proceedings of 6th World Conference on Earthquake Engineering*, New Delhi, India, **6**, 37-42.

2. Youd, T.L. and Perkins D.M. (1978) Mapping liquefaction-induced ground failure potential. *Journal of Geotechnical Engineering Division*, ASCE, **104**, 433-446.

3. Seed, H.B. (1979) Soil liquefaction and cyclic mobility evaluation for level ground during earthquakes. *Journal of Geotechnical Engineering Division*, ASCE, **105**(2), 201-255.

4. Kokusho, T., Yoshida, Y., Nishi, K., and Esashi, Y. (1983) *Evaluation of Seismic Stability of Sand Layer (part 1), Report 383025*. Electric Power Central Research Institute (in Japanese).

5. Troncoso, J., Ishihara, K., and Verdugo, R. (1988) Aging effects on cyclic shear strength of tailings materials. *Proceedings of Ninth World Conference on Earthquake Engineering*, Tokyo-Kyoto, Japan.

6. Andrus, R. and Stokoe II, K. (2000) Liquefaction Resistance of Soils from Shear-Wave Velocity. *Journal of Geotechnical and Geoenvironmental Engineering*, ASCE, **126**(11), 1015-1025.

7. Kayen, R.E., Seed, R.B., Moss, R.E.S., Cetin, K.O., Tokimatsu, K. and Tanaka, Y. (2004) Global shear wave velocity database for probabilistic assessment of the initiation of seismic-soil liquefaction. *11th International Conference on Soil Dynamics and Earthquake Engineering*.

8. Zhou, T.G. and Chen, T.M. (2007) Laboratory investigation on assessing liquefaction resistance of sandy soils by shear wave velocity. *Journal of Geotechnical and Geoenvironmental Engineering*, ASCE, **133**(8), 959-972.

9. Baxter, C., Bradshaw, A., Green, R., and Wang, J. (2008) A new correlation between cyclic resistance and shear wave velocity for silts. *Journal of Geotechnical and Geoenvironmental Engineering*, ASCE, **134**(1), 37-46.

10. Kayen, R., Moss, R.E.S., Thompson, E.M., Seed, R.B., Cetin, K.O., Kiureghian, A.D., Tanaka, Y. and Tokimatsu, K. (2013) Shear-wave velocity-based probabilistic and deterministic assessment of seismic soil liquefaction potential. *J. Geotech. Geoenviron. Engng.*, **139**(3), 407-419

.

11. Ishihara, K., Ueno, K., Yamada, S., Yasuda, S., and Yoneoka, T. (2015) Breach of a tailings dam in the 2011 earthquake in Japan. *International Journal of Soil Dynamics and Earthquake Engineering*, **68**, 3-22.

12. Robertson, P.K., Woeller, D.J., and Finn, W.D.L. (1992) Seismic cone penetration test for evaluating liquefaction potential under cyclic loading. *Canadian Geotechnical Journal*, **29**, 686-695.

13. Tokimatsu, K. and Uchida, A. (1990) Correlation between liquefaction resistance and shear wave velocity. *Soils and Foundations, Journal of Japanese Geotechnical Society*, **30**(2), 33-42.

14. Lodge, A.L. (1994) *Shear Wave Velocity Measurements for Subsurface Characterization*. PhD dissertation, University of California, Berkeley, California

15. Kayen, R.E., Mitchell, J.K., Seed, R.B., Lodge, A., Nishio, S., and Coutinho, R. (1992). Evaluation of SPT-, CPT-, and shear wave-based methods for liquefaction potential assessment using Loma Prieta data. *Proc., 4th Japan-U.S. Workshop on Earthquake Resistant Des. of Lifeline Fac. and Countermeasures for Soil Liquefaction*, Tech. Rep. NCEER-92-0019, Hamada, M. and O'Rourke, T.D. eds., **1**, National Center for Earthquake Engineering Research, Buffalo, 177-204.